Extension of the Injected-Absorbed-Current Method applied to DC-DC converters

Diego Ochoa, Antonio Lázaro, Marina Sanz, Andrés Barrado
Power Electronics System Group (GSEP)
Universidad Carlos III de Madrid (UC3M)
Leganes (Madrid), Spain
dochoa@ing.uc3m.es

Jorge Rodriguez
Deparment of Engineering
Power Smart Control SL
Leganes (Madrid), Spain
jorge.rodriguez@powersmartcontrol.com

***Abstract*—Sometimes a post-filter is implemented at the output of the converter, as there are applications that require a very low output voltage ripple or output current ripple. On the other hand, the use of an LC filter at the input of the converter is implemented with the aim of reducing electromagnetic interference or due to special specifications. As it is well known the implementation of both filters affect the dynamics of the system, therefore it is important to have the transfer functions that consider the effect of both filters in order to have an optimal design of the compensator and guarantee the stability of the system. In the existing literature, the effects of the input filter and post-filter have been addressed separately, the main objective of this paper is to analyze the dynamics of the system and extend the canonical model in order to obtain general transfer functions such as control to output voltage that involve the effect of both filters and even considering the feedforward of output current and input voltage. The phase-shifted full-bridge converter has been selected in order to validate the control to output voltage transfer function in an experimental and simulated way.**

Keywords—canonical model, dc-dc converters, input filter, output post-filter, phase-shifted full-bridge converter.

I. INTRODUCTION

In most of the telecommunications applications, it is required that the power supply keeps a very small variation or ripple in the output voltage of the power converter, for this reason one of the most used strategies in order to obtain a small output voltage ripple is the implementation of an output post-filter or a second stage of the LC filter in buck converter and its derived topologies [1]. On the other hand, the implementation of the LC filter at the input of the converter is very common, since it allows filtering the harmonics produced in the current due to the switching.

In the existing literature, it is well known that having power converters connected in cascade or the interaction between the input filter and the negative resistance obtained in the input impedance of a regulated converter that behaves as constant power load generates stability problems [2]-[3]. In [4] there is a review of some of the stability criteria applied to these types of systems. These criteria have in common that is necessary to know the magnitude and phase of the closed-loop input impedance and closed-loop output impedance of the converter in order to guarantee the stability of the system. Additionally, in some applications, the feedforward (FF) techniques are used to improve the transient response of the system by rejecting perturbations of the input voltage and output current [5]. Since the closed-loop input impedance and closed-loop output impedance depend on the control architecture, it is very important to consider the effects of the input voltage and output current feedforward when applying the stability criteria presented in [4]. Usually, all these effects (input filter, output post-filter and feedforward technique) have been analyzed separately.

In [6] the implementation of the output current and input voltage feedforward in the phase-shifted full-bridge converter is analyzed, however the effects that both filters produce on the control to output voltage transfer function are not analyzed. On the other hand, in [1] there is an analysis of the dynamics of the system with a second stage of the output filter, the transfer functions are proposed for a particular case as it is for the buck converter. Therefore, the advantage of working with the injected-absorbed current method is that the models can be applied to any type of converter. In its original version, the transfer functions presented in [7]-[9] have not been obtain taking into account the effect of the output post-filter, hence, it is important to extend the canonical model, since the control to output voltage transfer function is affected by the output post-filter, the feedforward of the output current and input voltage.

This paper shows how to obtain the control to output voltage transfer function in order to accurately analyze the dynamics of the system and thus be able to design an optimal compensator and guarantee the stability of the system.

Obtaining the transfer functions considering all the mentioned effects is a very complicated process, so this paper shows transfer functions starting from the basic characteristic coefficients (A_i, B_i, C_i, A_o, B_o, C_o) as these terms are well known in the literature. In addition, these transfer functions can be applied to different types of loads, such as resistive loads, constant power loads and batteries.

Finally, as an example to validate the transfer functions the phase-shifted full-bridge converter has been selected. The validation will be done by simulation using PSIM software [10] and experimentally using a frequency response analyzer from Venable instruments.

II. Extended Canonical Model

The coefficients of the input and output port of the converter without considering the input and output post-filter are represented by (1) and (2). Therefore, these expressions correspond to the classical model of the injected-absorbed current method [9].

$$\hat{\imath}_x = A_o(s)\cdot\hat{d} - B_o(s)\cdot\hat{v}_{oc} + C_o(s)\cdot\hat{v}_{in} \tag{1}$$

$$\hat{\imath}_m = A_i(s)\cdot\hat{d} - B_i(s)\cdot\hat{v}_{oc} + C_i(s)\cdot\hat{v}_{in} \tag{2}$$

In Fig. 1, the extension of the canonical model can be observed. The expressions (3), (4), (5), (6) and (7) are obtained from the equivalent circuit of the Fig. 1.

$$A_o(s)\cdot\hat{d} + C_o(s)\cdot\hat{v}_{in}(s) = \hat{\imath}_{oc}(s) + \frac{\hat{v}_{oc}(s)}{Z_{oc}(s)} \tag{3}$$

$$Z_{oc}(s) = \frac{1}{B_o(s)} \parallel Z_{Cfo}(s) \tag{4}$$

$$\hat{v}_{oc}(s) = \hat{\imath}_{oc}(s)\cdot Z_{Lp}(s) + \hat{v}_o(s) \tag{5}$$

$$\hat{\imath}_{oc}(s) = \hat{\imath}_o(s) + \frac{\hat{v}_o(s)}{Z_{Cp}(s)} \tag{6}$$

$$Z_g(s) = Z_{Li}(s) \parallel Z_{Ci}(s) \tag{7}$$

From the previous expressions, the new coefficients that consider the effect of the post-filter are obtained. The main advantage of this modeling technique is that by knowing the characteristic coefficients of the converter without considering the post-filter, the new coefficients of the canonical model presented in Table I are obtained quickly and directly, which consider the effect of the post-filter.

The criterion presented in [7], [8], [9] and [11] can be used to obtain the optimum feedforward compensation of the output current and input voltage. Therefore, for the case of the function $F_i(s)$ it can be observed in (8) as it is not affected by the post-filter. The term "G_m" represents the gain of the modulator.

$$F_i(s) = -\frac{C_o'(s)}{A_o'(s)\cdot G_m} = -\frac{C_o(s)}{A_o(s)\cdot G_m} \tag{8}$$

However, in the case of the function $F_o(s)$ that represents the optimum feedforward of the output current, it is affected by the post-filter as can be seen in (9).

$$F_o(s) = \frac{1}{A_o'(s)\cdot G_m} = \frac{Z_{oc}(s)\cdot Z_{Lp}(s)}{A_o(s)\cdot G_m\cdot Z_{oc}(s)} \tag{9}$$

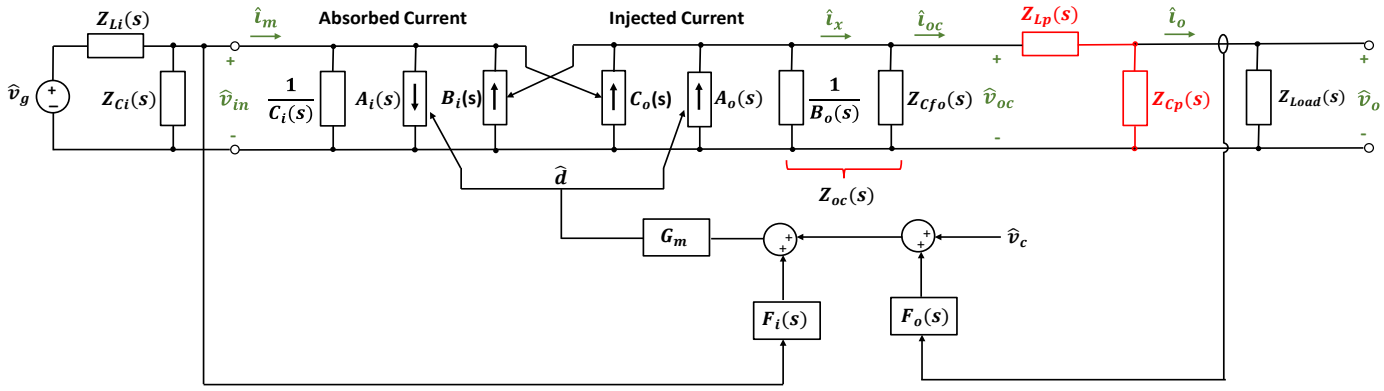

Fig. 1. Canonical model with input filter, output post-filter and feedforward compensations.

TABLE I: Coefficients of the canonical model considering output post-filter.

$A_o'(s) = \dfrac{A_o(s)}{1+\dfrac{Z_{Lp}(s)}{Z_{oc}(s)}}$	$B_o'(s) = \dfrac{\dfrac{1}{Z_{Cp(s)}} + \dfrac{Z_{Lp}(s)}{Z_{oc}(s)\cdot Z_{Cp}(s)} + \dfrac{1}{Z_{oc}(s)}}{1+\dfrac{Z_{Lp}(s)}{Z_{oc}(s)}}$
$C_o'(s) = \dfrac{C_o(s)}{1+\dfrac{Z_{LP}(s)}{Z_{oc}(s)}}$	$A_i'(s) = A_i(s) - \dfrac{B_i(s)\cdot Z_{Lp}(s)\cdot A_o(s)}{1+\dfrac{Z_{Lp}(s)}{Z_{oc}(s)}}$
$B_i'(s) = \dfrac{B_i(s)}{1+\dfrac{Z_{Lp}(s)}{Z_{oc}(s)}}$	$C_i'(s) = C_i(s) - \dfrac{B_i(s)\cdot Z_{Lp}(s)\cdot C_o(s)}{1+\dfrac{Z_{Lp}(s)}{Z_{oc}(s)}}$

Once the new coefficients have been obtained, the different transfer functions can be acquired, such as the closed-loop input impedance, closed-loop output impedance, audio-susceptibility and control to output voltage. As an example, in this paper, only control to output voltage transfer function ($G_{vvc}(s)$) is shown. It should be noted that (10) considers the effect of the input filter, post-filter and takes into account the two feedforward functions ($F_i(s)$ and $F_o(s)$). So that if the FF is not implemented, then set to zero the terms $F_i(s)$ and $F_o(s)$ to obtain the equivalent transfer function. Set to zero the term $Z_g(s)$ if it wants to obtain the equivalent control to output voltage transfer function when there is no input filter. The terms $Z_g(s)$ is given by (7) and it represents equivalent output impedance of the input filter.

III. Small Signal Model of Phase-Shifted Full-Bridge Converter

From the steady-state analysis of Phase-Shifted Full-Bridge converter (PSFB) presented in [12], it should be noted that the voltage at the secondary of the transformer is not determined by the duty cycle (D) that is imposed by the control loop, but it depends on the effective duty cycle (D_{eff}), since the leakage inductor (L_{lk}) of the transformer generates a voltage drop or reduction of the duty cycle. These effects are represented by (11), (12), (13) and (14).

$$D = \Delta D + D_{eff} \tag{11}$$

$$D_{eff} = \frac{V_o}{n \cdot V_{in}} \tag{12}$$

$$\Delta D = \frac{R_d}{2 \cdot n \cdot V_{in}} \cdot \left(2 \cdot I_{Lfo} - \frac{V_o}{L_{fo}} \cdot (1 - D) \cdot \frac{T_{sw}}{2}\right) \tag{13}$$

$$R_d = 4 \cdot n^2 \cdot L_{lk} \cdot F_{sw} \tag{14}$$

The term "I_{Lfo}" is the output filter inductor current, "n" represents the turn ratio of the transformer, "L_{lk}" is the leakage inductance of the transformer, "V_o" is the output voltage, L_{fo} is the output filter inductance and "F_{sw}" is the switching frequency. In [13] the small signal model of the phase-shifted full-bridge converter is proposed based on the small signal model of the buck converter. Also, in [13] it is mentioned that the duty cycle is affected by the perturbation of the output filter inductor current and the perturbation of the input voltage. However, it is necessary to take into account the duty cycle is also perturbed by the output voltage in order to have a complete model. By applying (15) and replacing in (11) it gets the new expressions that are shown in (16), (17), (18) and (19).

$$\Delta\hat{d} = \frac{\partial \Delta D}{\partial d} \cdot \hat{d} + \frac{\partial \Delta D}{\partial V_{in}} \cdot \hat{v}_{in} + \frac{\partial \Delta D}{\partial I_{Lfo}} \cdot \hat{\imath}_{Lfo} + \frac{\partial \Delta D}{\partial V_o} \cdot \hat{v}_o \tag{15}$$

$$\hat{d}_d = -\frac{R_d \cdot V_o \cdot T_{sw}}{4 \cdot n \cdot V_{in} \cdot L_{fo}} \cdot \hat{d} \tag{16}$$

$$\hat{d}_i = -\frac{R_d}{n \cdot V_{in}} \cdot \hat{\imath}_{Lfo} \tag{17}$$

$$\hat{d}_{vi} = \frac{R_d}{2 \cdot n \cdot V_{in}^2} \cdot \left(2 \cdot I_{Lfo} - \frac{V_o}{L_{fo}} \cdot (1 - D) \cdot \frac{T_{sw}}{2}\right) \hat{v}_{in} \tag{18}$$

$$\hat{d}_{vo} = \frac{R_d \cdot (1 - D) \cdot T_{sw}}{4 \cdot n \cdot V_{in} \cdot L_{fo}} \cdot \hat{v}_o \tag{19}$$

Finally, by replacing the duty cycle of the classical buck converter with the effective duty cycle generated in the secondary of the PSFB, then the circuit of Fig. 2 is obtained. From this equivalent circuit, the current through the output filter inductor ($\hat{\imath}_{Lfo}$) and the input current ($\hat{\imath}_{in}$) can be calculated based on duty cycle perturbation ($\hat{d}$), output voltage perturbation ($\hat{v}_o$) and input voltage perturbation ($\hat{v}_{in}$) in order to know the characteristic coefficients of the injected-absorbed current method. The expressions (20), (21) and (22) are given from the output port of the converter.

$$A_o(s) = \frac{n \cdot V_{in} \cdot \left(1 - \frac{R_d \cdot V_o \cdot T_{sw}}{4 \cdot n \cdot V_{in} \cdot L_{fo}}\right)}{Z_{Lfo}(s) + R_d} \tag{20}$$

$$B_o(s) = \frac{1 - \frac{R_d \cdot (1 - D) \cdot T_{sw}}{4 \cdot L_{fo}}}{Z_{Lfo}(s) + R_d} \tag{21}$$

$$C_o(s) = \frac{n \cdot D_{eff} + \frac{R_d}{2 \cdot V_{in}} \cdot \left(2 \cdot I_{Lfo} - \frac{V_o}{L_{fo}} \cdot (1 - D) \cdot \frac{T_{sw}}{2}\right)}{Z_{Lfo}(s) + R_d} \tag{22}$$

The expressions (23), (24) and (25) are given from the input port of the converter.

$$A_i(s) = \frac{\left(I_{Lfo} \cdot Z_{Lfo}(s) + D_{eff} \cdot n \cdot V_{in}\right) \cdot \left(4 \cdot L_{fo} \cdot V_{in} \cdot n - R_d \cdot T_{sw} \cdot V_o\right)}{4 \cdot L_{fo} \cdot V_{in} \cdot \left(Z_{Lfo}(s) + R_d\right)} \tag{23}$$

$$G_{vvc}(s) = \frac{A'_o(s) \cdot G_m - \frac{\left(A'_o(s) \cdot G_m \cdot F_i(s) + C'_o(s)\right) \cdot Z_g(s) \cdot G_m \cdot A'_i(s)}{1 + Z_g(s) \cdot C'_i(s) + Z_g(s) \cdot G_m \cdot A'_i(s) \cdot F_i(s)}}{\frac{1}{Z_{load}(s)} + B'_o(s) - \frac{A'_o(s) \cdot G_m \cdot F_o(s)}{Z_{load}(s)} - \frac{Z_g(s) \cdot \left(A'_o(s) \cdot G_m \cdot F_i(s) + C'_o(s)\right) \cdot \left(B'_i(s) - \frac{A'_i(s) \cdot G_m \cdot F_o(s)}{Z_{load}(s)}\right)}{1 + Z_g(s) \cdot C'_i(s) + Z_g(s) \cdot G_m \cdot A'_i(s) \cdot F_i(s)}} \tag{10}$$

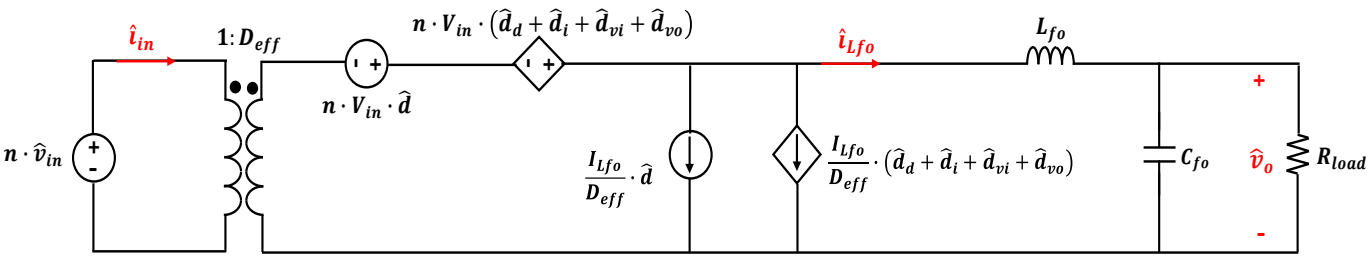

Fig. 2. Small signal model of phase-shifted full bridge converter by approximation to the buck converter.

$$B_i(s) = B_o(s) \cdot \left(n \cdot D_{eff} - \frac{R_d \cdot I_{Lfo}}{V_{in}}\right) - I_{Lfo} \cdot \left(\frac{R_d \cdot (1-D) \cdot T_{sw}}{4 \cdot V_{in} \cdot L_{fo}}\right) \quad (24)$$

$$C_i(s) = C_o(s) \cdot \left(n \cdot D_{eff} - \frac{R_d \cdot I_{Lfo}}{V_{in}}\right) + \frac{I_{Lfo} \cdot R_d}{2 \cdot V_{in}^2} \cdot \left(2 \cdot I_{Lfo} - \frac{V_o}{L_{fo}} \cdot (1-D) \cdot \frac{T_{sw}}{2}\right) \quad (25)$$

Once the characteristic coefficients of the converter have been determined, the new coefficients that consider the effect of the output post-filter ($A_i'(s)$, $B_i'(s)$, $C_i'(s)$, $A'_o(s)$, $B'_o(s)$, $C'_o(s)$) can be easily obtained and thus be able to use the expression that allows obtaining the frequency response of the control to output voltage transfer function ($G_{vvc}(s)$).

IV. Validation by Simulation

In order to validate the model of the Phase-Shifted Full-Bridge converter with output post-filter and input filter, the frequency response is analyzed using the "Ac-sweep" function of PSIM. The main parameters of the Phase-Shifted Full-Bridge converter are in Table II. The schematic of PSIM is shown in Fig. 3.

The theoretical and simulated frequency response is compared in Fig. 4. From Fig. 4, it can be seen how the resonance frequency of the input filter is around the value of 40 kHz, which complies with the expression (26). The effect of the input filter is slightly dampened due to the parasitic components of the inductor (L_i) and capacitor (C_i).

$$f_{R,if} = \frac{1}{2 \cdot \pi \cdot \sqrt{L_i \cdot C_i}} \quad (26)$$

TABLE II: Parameters of the converter.

Parameter	Value
Input Voltage (V_{in})	40 V
Output Voltage (V_o)	6.7 V
Switching frequency (F_{sw})	100 kHz
Output filter inductance (L_{fo})	36 uH
Transformer turn ratio (n)	0.5
Output filter capacitance (C_{fo})	880 nF
Leakage inductance (L_{lk})	4.61 uH
Load resistor (R_{load})	1.7 ohm
Output post-filter capacitance (C_p)	22 uF
Output post-filter inductance (L_p)	10 uH
Input filter capacitance (C_i)	4.3 uF
Input filter inductance (L_i)	3.3 uH
Output capacitance of MOSFET (c_{oss})	60 pF

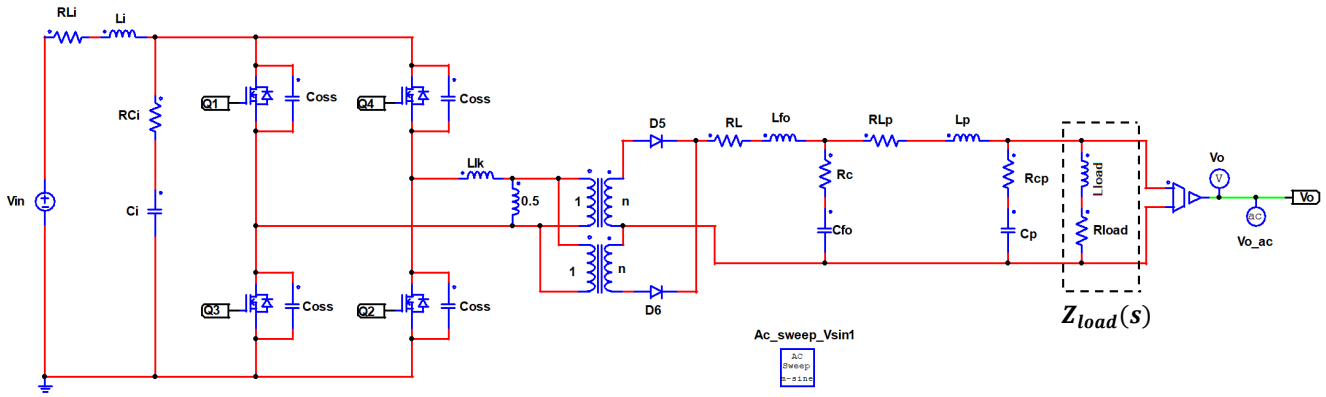

Fig. 3. PSIM schematic of phase-shifted full-bridge converter with input filter and output post-filter.

On the other hand, there is a second resonance peak whose frequency is around of 60 kHz. This resonance is determined by the combination of the first and second stage of the LC filter at the output of the converter. Finally, as the converter is controlled by a digital platform, the respective delay must be compensated.

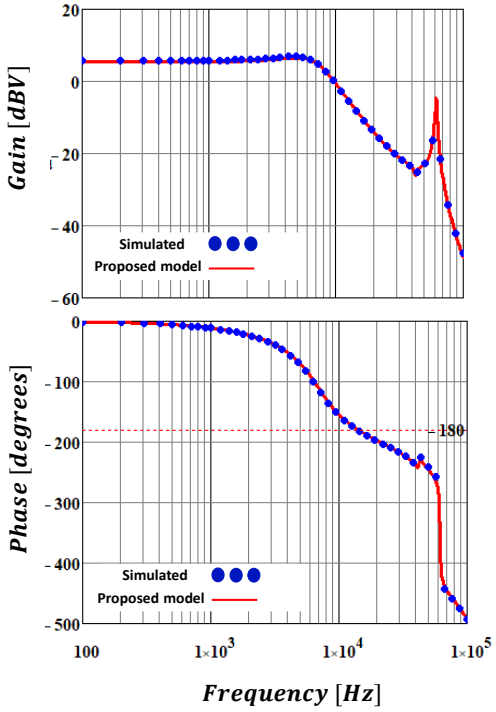

Fig. 4. Simulated and theoretical frequency reponse of G_{vvc} transfer function with output post-filter, and input filter.

V. Experimental Results

The converter is controlled by a system on chip (SoC) of Z-7020 Xilinx Zynq device [14]. The frequency response is obtaining by using the Venable frequency response analyzer. The experimental prototype used to validate the frequency response of the control to output voltage transfer function is in Fig. 5.

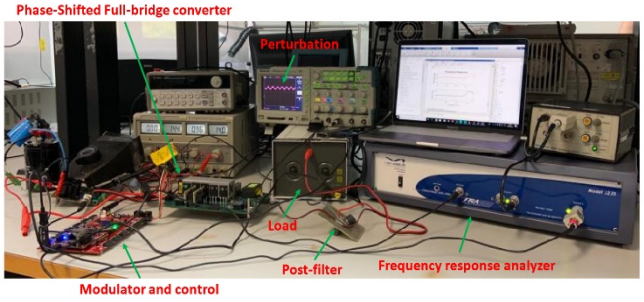

Fig. 5. Experimental prototype of phase-shifted full-bridge converter.

The main waveforms of the converter (the primary voltage of the transformer, the rectified voltage and the output current) are shown in Fig. 6. Finally, Fig. 7 shows the magnitude and phase of the frequency response of the system measured experimentally.

It can be emphasized that the experimental measurement fits with the theoretical predictions. The small differences that exist in the frequency response is due to the parasitic element and power losses.

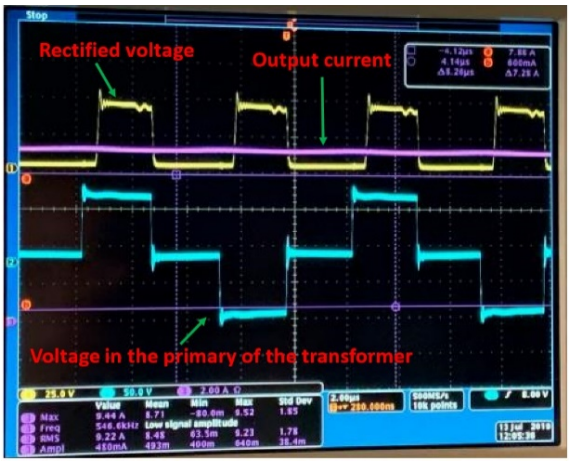

Fig. 6. Main waveforms of phase-shifted full-bridge converter.

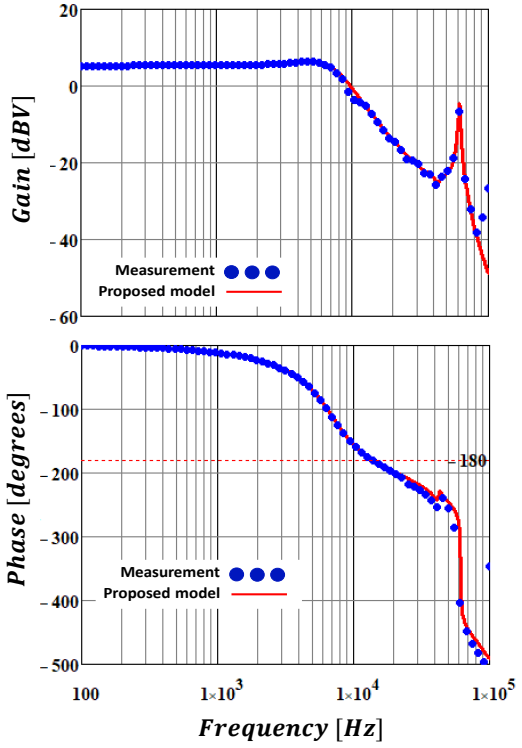

Fig. 7. Experimental and theoretical frequency reponse of G_{vvc} transfer function with output post-filter and input filter.

VI. Conclusions

An extension of the injected-absorbed current method is proposed that consider the effects of the input filter, output post-filter, feedforward compensations and various types of loads. This extension allows to obtain very complicated transfer functions based on the very simple and well-known expressions of the converter operating alone (without both filters). These transfer functions can be easily programmed by some software.

From the proposed model, it can very quickly obtain the transfer functions necessary to analyze the stability criteria that guarantee the stability of the converters that are connected in cascade. On the other hand, the small signal model of the Phase-Shifted Full-Bridge converter has been completed by approximation of the buck converter.

ACKNOWLEDGMENT

This work is partially supported by the European Regional Development Fund, the Ministry of Science, Innovation and Universities and the State Research Agency through the research projects “Modelling and control strategies for the stabilization of the interconnection of power electronic converters”-CONEXPOT-2-(DPI2017-84572-C2-2-R) (AEI/FEDER, UE).

REFERENCES

[1] M. Orabi, “Voltage Deviation of POL Converter with Two-Stage Output Filter”, IEEE Aplied Power Electronics Conference and Exposition (APEC), 2011.

[2] Mingfei Wu, and Dylan Dah-Chuan Lu, “A Novel Stabilization Method of LC Input Filter With Constant Power Loads Without Load Performance Compromise in DC Microgrids,” IEEE Transactions on Industrial Electronics, vol. 62, no. 7, pp. 4552-4562, Jul 2015.

[3] R. D. Middlebrook, “Input Filter consideration in design and application of switching regulators”, in Proc. IEEE Ind. Applicat. Soc. Annu. Meeting, 1976.

[4] A. Riccobono, E. Santi, “Comprehensive Review of Stability Criteria for DC Power Distribution Systems”, IEEE Transactions on Industry Applications, vol. 50, no. 5, pp. 3525-3535, Sept 2014.

[5] Yao. Chuan, X. Ruan, and X. Wang, “Automatic Mode Shifting Control Strategy With Input Voltage Feed-Forward for Full-Bridge-Boost DC-DC Converter Suitable for Wide Input Voltage Range”, IEEE Transactions on Power, vol. 30, no. 3, pp. 1668-1682, March 205.

[6] Z. Jiaxing, W. Yong, and Y. Fanhe, “Dual Feedforward Closed-Loop Control for Phase-Shifted Full Bridge DC-DC Converter”, IEEE Asia Power and Energy Engineering Conference (APEEC), 2019.

[7] R. Redl and N. O. Sokal, “Optimizing dynamic behavoir with input and output-feedforward and current-mode control”, in Proc. Powercon7, San Diego, CA, USA, 1980, pp. H1-1-H1-16.

[8] R. Redl and N. O. Sokal, “Near-optimum dynamic regulation of dc-dc converters using feed-forward of output current and input voltage with current-mode control,”, IEEE Trans. Power Electron., vol. PE-1, no. 3, pp. 181-192, Jul. 1986.

[9] A. Kislovski, R. Redl, N. O. Sokal, “Dynamic Analysis of Switching-Mode DC/DC Converters”, Springer Science & Business Media, 2012.

[10] Psim User’s Guide, Ver.11.1, July, 2018, POWERSYM.

[11] B. Wang, P. Jia, T. Zhenq, Y. Li, “Research on Stability of Buck Converter with Output-Current-Feedforward Control”, IEEE Applied Power Electronics Conference and Exposition (APEC), 2014.

[12] J. Sabate, V. Vlatkovic, R. Ridley, F. Lee and B. Cho, “Design considerations for high-voltage high-power full-bridge zero-voltage-switched PWM converter”, IEEE Applied Power Electronics Conference and Exposition (APEC), 1990, pp. 275-284.

[13] V. Vlatkovic, J.A. Sabate, R. Ridley, F. Lee and B. Cho, “Small-signal analysis of the phase-shifted PWM converter”, IEEE Transaction on power Electronics, vol. 7, no. 1, pp. 128-135, 1992.

[14] Zynq-7000 All Programmable SOC Technical Reference Manual, UG585 (v1.10), Xilinx, San Jose, CA, USA, Feb 2015.